

## Chloride and Sulfate Resistance of Calcined Lateritic Clay-Based Geopolymer

<sup>1,2</sup>Usman Ghani\*, <sup>1,2</sup>Shah Hussain, <sup>1</sup>Noor ul Amin\*, <sup>2</sup>Maria Imtiaz, <sup>3</sup>Shahid Ali Khan, <sup>2</sup>Muhammad Naeem

<sup>1</sup>Department of Chemistry, Abdul Wali Khan University Mardan, Pakistan.

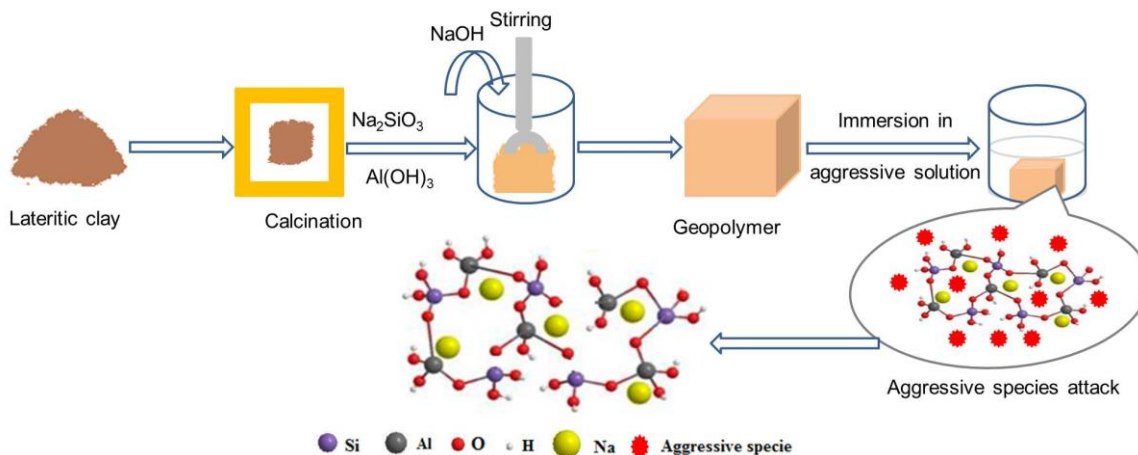
<sup>2</sup>Department of Chemistry, Government Postgraduate College Nowshera, Pakistan.

<sup>3</sup>Department of Chemistry, School of Natural Sciences, National University of Science and Technology (NUST), Islamabad, Pakistan.

[noorulamin@awkum.edu.pk](mailto:noorulamin@awkum.edu.pk); [usmanap19@yahoo.com](mailto:usmanap19@yahoo.com)\*

(Received on 15<sup>th</sup> June 2021, accepted in revised form 1<sup>st</sup> November 2021)

**Summary:** The dissemination of chloride and sulfate ions greatly affects the quality and strength of concrete obtained from cementitious materials. The current research is focused on the development of good quality geopolymer from calcined lateritic clay, sodium metasilicate, and aluminum hydroxide with optimum Si to Al ratio (by mass) and study of its resistance in aggressive environments of chloride and sulfate. Different geopolymer samples with Si to Al ratio of 3 to 1 were prepared and exposed in 8 wt.% sodium chloride and sodium sulfate solutions for 7, 14, 21, 28, and 35 days. The geopolymer sample with Si to Al ratio = 1.5 offers greater resistance in aggressive environments. The resistance of geopolymer remained better in sodium chloride solution than in sodium sulfate solution. The reduction of compressive strength of the geopolymer is 7% less in sodium chloride solution than in sodium sulphate solution. FTIR and XRD investigation proved that both chloride and sulfate do not affect the bonding and structural features of geopolymer however slight erosion of the surface morphology confirmed by SEM analysis. It can be concluded that an impure clay can be utilized to obtain a valuable product.



**Keywords:** Lateritic clay, Calcination, Geopolymer, Compressive strength, Chloride & sulfate resistance.

### Introduction

Ordinary Portland Cement (OPC) as a binder is commonly used in the making of concrete and considered as long-lasting material. Unfortunately, the production process of OPC and resistance to aggressive environments like acids, chlorides, and sulfates are of major concern [1]. The production process releases a huge amount of greenhouse gases, causing global warming [2], while the attack by aggressive environments deteriorates the physical and mechanical properties of OPC-based concrete upon exposure for a long time [3]. To overcome these issues, different cement alternatives as binder are being introduced among which geopolymer gets great attention [4] due to its production process which is

environment friendly by releasing 80% less CO<sub>2</sub> gas to the atmosphere than OPC production [5] and offers greater resistance to aggressive environments [6].

Geopolymers are amorphous or semi-crystalline obtained by alkaline treatment of the rich source of aluminosilicate based materials including both solid industrial waste (ash) or natural minerals (kaolin) and subsequent curing at room or slightly high temperature [7]. The formation of a geopolymer completed in three steps i.e. first the alkaline activator dissolves the solid aluminosilicate oxide to form free tetrahedral units of SiO<sub>4</sub> and AlO<sub>4</sub><sup>-</sup>, followed by the polycondensation reaction of these free units to form

\*To whom all correspondence should be addressed.

the geopolymer gel. Whereas in the last step, the polymeric gel gets hardened gradually to yield geopolymers [4]. The resultant geopolymer is negatively charged due to  $\text{AlO}_4^-$  units balanced by alkali cation [8]. Most recently, some new aluminosilicate based potential raw materials including powdered banana peels [9], meta-halloysite [10], iron rich lateritic clay [11] and groundnut shell powder [12] are utilized to get good quality geopolymers.

The strength of OPC based concrete predominantly relies on basic calcium silicate hydrates and can easily be attacked by acids, sulfate, and chloride ions containing solutions whereas geopolymer based concrete gets their strength due to the polycondensation of  $\text{SiO}_4$  and  $\text{AlO}_4^-$  units forming three-dimensional network. This reaction gives greater stability to geopolymer concrete in different aggressive environments [13].

Tigue et al. 2018 [14] studied the behavior of fly ash and soil-based geopolymer in 5 wt.% sulphuric acid solution after immersion for 28 and 56 days and found a greater stability of geopolymer in an aggressive environment. Kwasny et al. 2018 [15] studied the durability of the mortars derived from calcined lithomarge and OPC in sulphate and acidic environments for 52 weeks and found a good performance of geopolymeric mortars over OPC mortars. Vafaei et al. 2019 [16] compared the durability of fly ash and calcium aluminate based geopolymer with OPC and high alumina cement-based mortar in hydrochloric acid and sulfuric acid solutions of  $\text{pH} = 3$  and observed that hydrochloric acid solution has a better performance than sulphuric acid solution. Shah et al. 2020 [17] studied the stability of geopolymer obtained from tile waste ceramic powder, fly ash, and ground blast furnace slag in a 10% sulphuric acid solution and reported its excellent performance in the acid attack. Most recently, Dongming et al. 2020 [18] reported the chemical, physical, and mechanical stability of a metakaolin based geopolymer in aggressive environment of sulfate ions. They immersed the geopolymer in sodium sulfate and magnesium sulfate solution for 180 days and observed substantial stability of geopolymer in a harsh environment.

The focus of the current investigation is to study the durability and stability of calcined lateritic clay-based geopolymer in aggressive environments of chloride and sulfate. None of the studies have yet reported the behavior of a calcined lateritic clay-based

geopolymer in chloride and sulfate immersion. Sodium chloride and sodium sulfate solutions were used as chloride and sulfate aggressive environments, respectively. Different geopolymers samples prepared with Si to Al ratio in the range of 1 to 3 by mixing calcined lateritic clay, sodium metasilicate, and aluminum hydroxide, were exposed to aggressive environments of chloride & sulfate and assessed their influence after immersion on their mass and compressive strengths.

## Experimental

### Materials

Lateritic clay sourced from Chashmai District Nowshera, Pakistan was calcined at 900 °C and employed as a precursor to prepare geopolymer. The chemical composition of lateritic clay was determined by X-ray Fluorescence (XRF) analysis using the Cubix XRF spectrometer (Model: PW2300, Netherland). Fine powder of sodium metasilicate and potassium hydroxide pellets of analytical grade procured from Sigma-Aldrich Co, St Louis, USA while analytical grade aluminum hydroxide powder was purchased from Riedel-de-Haen Co. USA.

### Geopolymer Synthesis

The calcined lateritic clay was fine grounded, sieved through 58  $\mu\text{m}$  mesh screen, and mechanically mixed with sodium metasilicate and aluminum hydroxide for 15 min to homogenize in a dry state. To synthesize a geopolymer, 6 M KOH solution was added slowly to the dry mixture with constant mechanical stirring until homogenization maintaining liquid to solid (mL/g) ratio at 0.5 which gives better workability. The resultant pastes were casted into cubic molds and cured for 1 day at 80°C. The hardened geopolymer samples were de-molded and again kept in the same conditions for 6 days. All the de-molded samples were labeled as LG1, LG2, LG3, LG4, and LG5 and stored in polythene bags at room temperature until the testing day. The composition of each geopolymer is given in Table-1.

Table-1: Dry state composition of geopolymer mixture.

Raw materials were taken	Weight Taken (%)				
	LG1	LG2	LG3	LG4	LG5
Clay	50.0	50.5	50.5	49.0	49.5
Aluminum hydroxide	10.0	13.8	18.3	26.4	38.2
Sodium silicate	40.0	35.7	31.2	24.6	12.3
Si to Al ratio	3.00	2.50	2.00	1.50	1.00

### Stability study of geopolymer

In instability study, dried geopolymer samples were exposed to chloride and sulfate environments by immersing in 8 wt.% sodium chloride and sodium sulfate solutions and placed at ambient conditions each for 7, 15, 21, 28, and 35 days. Finally, the effect of chloride and sulfate attack on geopolymer samples was assessed by measuring their loss in mass & compressive strength and change in bonding, morphological & mineralogical features.

### Characterization techniques

The loss in mass of geopolymer after immersion in aggressive environments relative to before immersion was computed by using the following equation:

$$\text{Loss in a mass of geopolymer (\%)} = \frac{m_1 - m_2}{m_1} \times 100 \quad (1)$$

where  $m_1$  and  $m_2$  are the masses of geopolymer before and after immersion in aggressive environments, respectively.

The compressive strength of all the geopolymer samples before and after immersion in chloride and sulfate environments for 7, 14, 21, 28, and 35 days of exposure was studied by using a universal testing machine (UTM) (Model: 100-500KN, Testometric Inc. UK).

The change in bonding features of geopolymers after immersion was evaluated by FT-IR spectroscopic studies and their spectra were collected over the wave number range of 4000 to 400  $\text{cm}^{-1}$  using FT-IR spectrophotometer (PerkinElmer Spectrum, Version 10.4.00).

The effect of aggressive environments on morphological features of geopolymer was investigated by scanning electron microscope (SEM) (Model JEOL-JSM-5910; Japan).

The mineralogical composition of geopolymers before and after immersion was evaluated by XRD analysis by using an X-ray diffractometer (JDX-9C, JOEL, Japan) using a 2-theta angle range from 10 to 70° at room temperature, with  $\text{CuK}\alpha$  radiation and a nickel filter.

## Results and Discussion

### Characterization of lateritic clay

The chemical composition of lateritic clay is provided in Table 2, indicating silica and alumina as major constituents contributing 80.98 wt.% of the sample. The low moisture content and loss on ignition (LOI) values are evidence of very low reactions of clay components upon calcination. Since silica and alumina are involved in making the main geopolymeric network,[19] therefore according to ASTM C311 method [20] the selected clay can be used as a good natural pozzolana for geopolymer production.

Table-2: Chemical composition of lateritic clay.

Wt.%								
SiO <sub>2</sub>	Al <sub>2</sub> O <sub>3</sub>	Fe <sub>2</sub> O <sub>3</sub>	CaO	MgO	K <sub>2</sub> O	Na <sub>2</sub> O	Moisture/ H <sub>2</sub> O	LOI
63.92	17.06	5.88	3.91	2.3	3.13	3.1	0.099	0.64

The FT-IR spectra of un-calcined and calcined lateritic clay samples given in Fig. 1 indicate the major peaks of Al-O of  $\text{AlO}_4^-$  and Si-O of  $\text{SiO}_4$  units. In the spectrum of the un-calcined clay sample provided in Fig. 1a, the peaks at 499 and 979  $\text{cm}^{-1}$  correspond to Al-O bonds bending vibrations of  $\text{AlO}_4^-$  units of kaolinite minerals [21], while peaks at 694 and 794  $\text{cm}^{-1}$  are associated with the vibration of Si-O bonds of  $\text{SiO}_4$  units [22]. The FT-IR spectrum of lateritic clay calcined at 900 °C given in Fig. 1b indicates the shifting of Al-O bond peaks of higher wave number and the appearance of the peaks of Si-O bonds at lower wave number with reducing intensities is evident of the transformation of aluminates and silicates into amorphous alumina and silica, respectively [23].

XRD pattern of lateritic clay used as geopolymer precursor indicated major diffraction peaks of quartz ( $\text{SiO}_2$ ), kaolinite ( $\text{Al}_2\text{O}_3(\text{SiO}_2)_2(\text{H}_2\text{O})_2$ ), hematite ( $\text{Fe}_2\text{O}_3$ ), and goethite ( $\text{Fe}(\text{OH})\text{O}$ ) in the range of 15 to 60° as shown in Fig. 2a. The XRD pattern of calcined lateritic clay provided in Fig. 2b shows changes in the intensity of various peaks. The Fig. 2b indicates decrease in the intensity of some quartz peaks, complete absence of kaolinite peaks, and goethite peaks being replaced by hematite [24]. The decrease in the quartz peaks intensities and the disappearance of kaolinite peaks is evidence of the formation of amorphous metakaolinite [25], and the transformation of goethite to hematite confirms the structural disorderness of calcined lateritic clay which makes it attractive for alkaline activation to synthesize geopolymer. The presence of quartz minerals must act as fillers due to their resistance to dissolve in an alkaline medium [19].

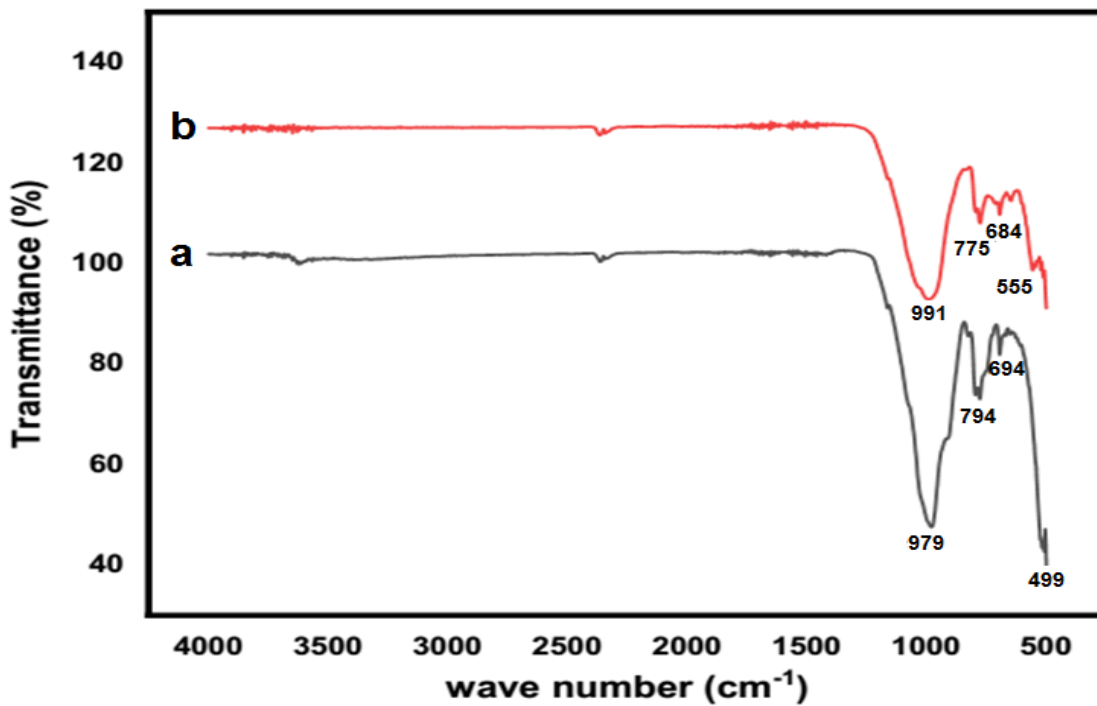


Fig. 1: FT-IR spectra of lateritic clay: before calcination (a) and after calcination (b).

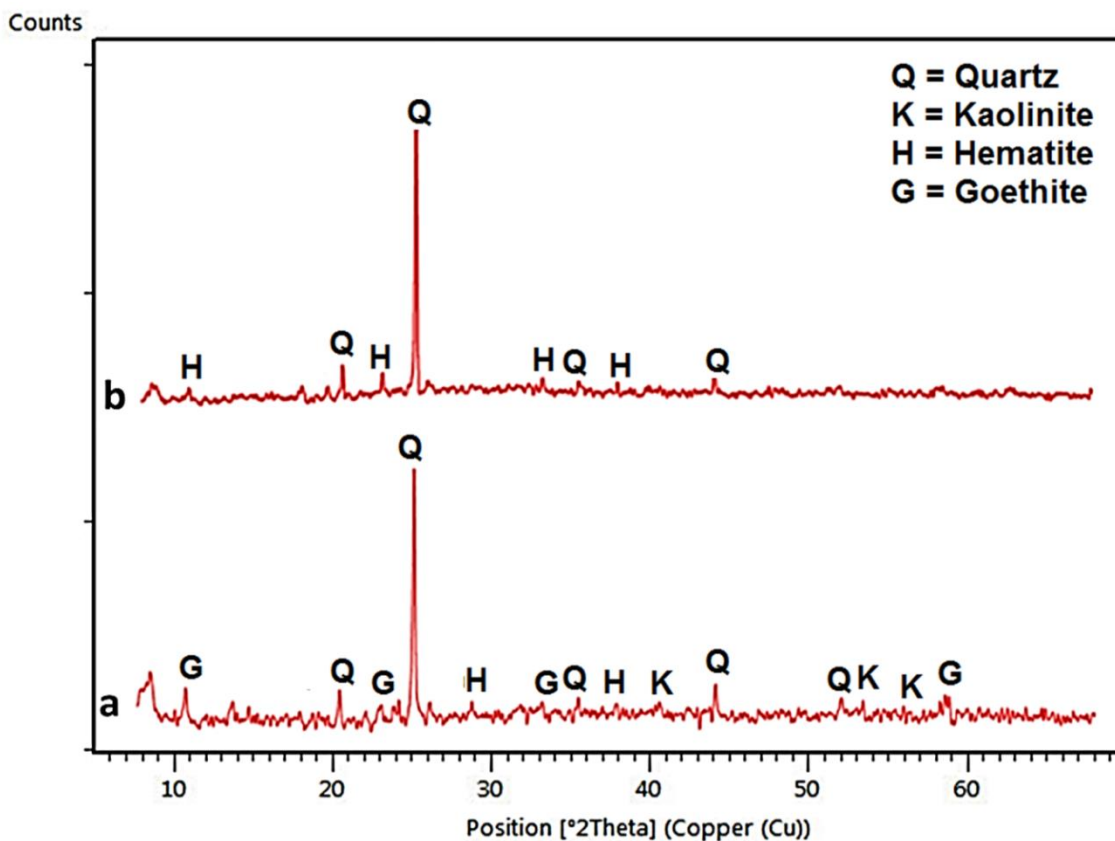


Fig. 2: XRD patterns of lateritic clay samples: un-calcined (a) and calcined at 900°C.

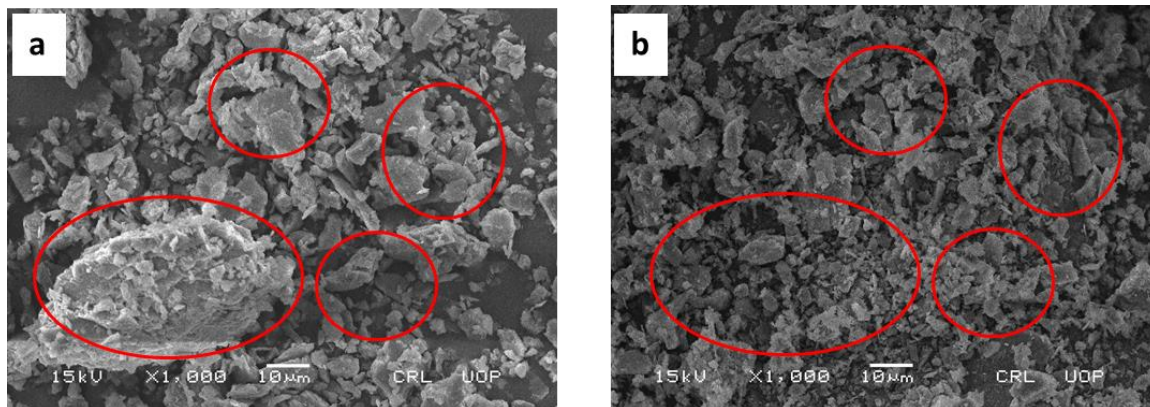


Fig. 3: SEM micrograph of lateritic clay samples: un-calcined (a) and calcined at 900°C (b).

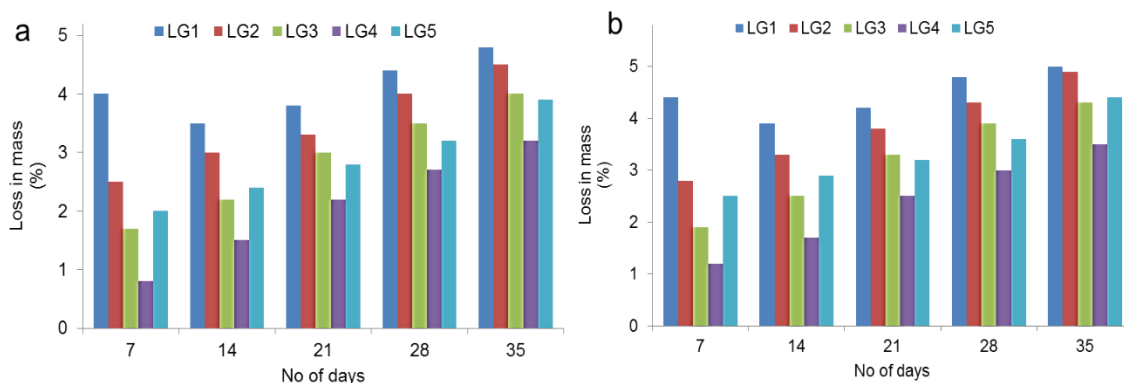


Fig. 4: Effect of immersion duration on the stability of geopolymer samples in: chloride (a) and sulphate (b) environments.

The SEM image of un-calcined lateritic clay is provided in Fig. 3. The subtle differences in morphology brought by calcination have been visualized with red circles. The micrograph of un-calcined clay given in Fig. 3a reveals the presence of flakes of different nano-sized detachment and uneven dispersion when calcined at 900 °C as depicted in Fig. 3b. The uneven dispersion of flakes confirms the structural disorderliness and transformation of clay components into amorphous phases.

*Characterization of geopolymer*  
*Loss in mass*

The stability of geopolymer samples with different mix proportions of calcined lateritic clay, sodium metasilicate, and aluminum hydroxide exposed to chloride and sulfate solutions was assessed in terms of loss in mass. Fig. 4 indicates the percent loss in mass of geopolymer samples due to immersion in 8 wt.% sodium chloride and sodium sulfate solutions for 7, 14, 21, 28, and 35 days. The data

clearly reveals that the stability of blended geopolymers increases as the Si to Al ratio decreases up to 1.5 and then decreases. The similar trend is also reported by Amin et. al., 2017 [1]. However, increasing contact time with an aggressive environment resulted in a greater loss in the mass of geopolymer samples. The percent loss in mass of geopolymer samples LG1, LG2, LG3, LG4, and LG5 in the chloride environment remained 4.8, 4.5, 4, 3.2 & 3.9% and in the sulfate environment, it remained 5, 4.9, 4.3, 3.5, and 4.4%, respectively after 35 days of immersion. The change in mass of geopolymer may reflect depolymerization which lowered the quality of geopolymer whereas resistance offered might be due to a greater degree of polymerization and greater filler effect of silica and alumina present in calcined lateritic clay sample[13]. The results indicated that LG4 shows greater stability in chloride and sulfate environments. Overall erosion effect of sulfate solution is greater than the chloride solution show close agreement with the results reported by Ahmet et al.2019 [26].

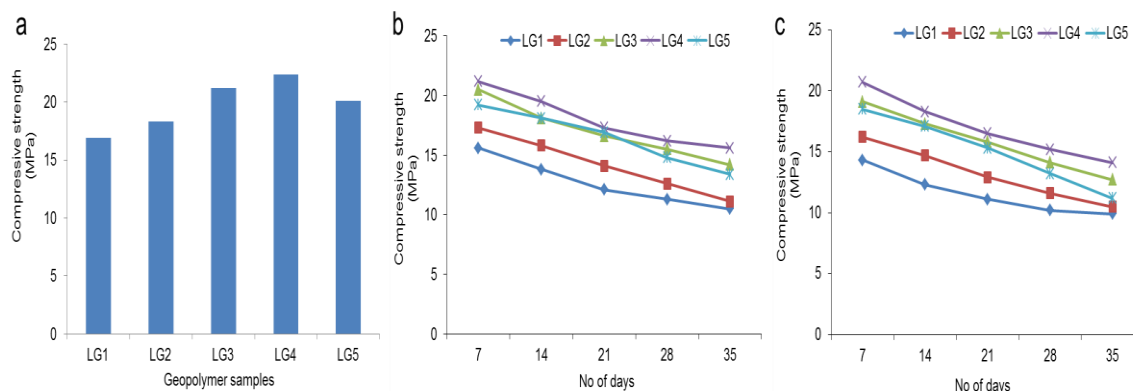


Fig. 5: Compressive strength of geopolymer samples: Before immersion (a), after immersion in chloride environment (b) and after immersion in sulfate environment (c).

#### *Effect of chloride and sulphate environments on compressive strength*

The stability of calcined lateritic clay-based geopolymer blended with sodium metasilicate and aluminum hydroxide was also examined by investigating the effect of chloride and sulfate environments on the compressive strength. According to Amin et al. 2017 [1], the excellent compressive strength of the geopolymer can be achieved by mixing raw materials at an exact stoichiometric ratio of Si and Al. Fig. 5 shows the effect of various Si to Al ratio on the compressive strength of geopolymer samples before and after immersion in 8 wt.% sodium chloride and sodium sulfate solutions for 7, 14, 21, 28, and 35 days. The highest compressive strength of 22.4 MPa was obtained for LG4 sample. The change in compressive strength of samples by chloride and sulfate attack has found a similar trend as loss in mass. Fig. 5b and 5c shows that the LG4 sample performs better than other geopolymer samples upon exposure to aggressive environments. However, for all samples, a slight reduction of compressive strength was observed. The mechanism involved in the reduction of compressive strength is the attack of aggressive species of a solution on geopolymeric bonds causing deterioration in the geopolymeric structures [27] whereas the excellent performance by the geopolymer samples against chloride and sulfate environment may be attributed to the stable structure of geopolymer formed due to utilization of sodium silicate which provides soluble Si leading to better geopolymerization [28].

#### *FT-IR spectroscopic analysis*

The effect of aggressive environments on the bonding network of geopolymer at optimal Si to Al ratio was studied by collecting FT-IR spectra provided in Fig. 6. The major peaks in the FT-IR spectrum of

the geopolymer shown in Fig. 6a appeared at 3526, 3452, 1021, 945, 763, 670 and, 559  $\text{cm}^{-1}$ . The peaks at 3526 and 3426  $\text{cm}^{-1}$  are due to the O-H stretching vibration of the silanol (Si-OH) group [29]. The bands appeared in the ranges: 940 to 1030  $\text{cm}^{-1}$ ; 550 to 565  $\text{cm}^{-1}$  and at 763  $\text{cm}^{-1}$  demonstrated the symmetric & asymmetric stretching and bending vibrations of Si-O-Si and Si-O-Al bonds described as the main characteristic bond of a geopolymeric network[30]. The peak at 670  $\text{cm}^{-1}$  is correlated to the Si-O-Fe bond give an indication of the participation of calcined lateritic clay iron in geopolymerization[31]. All characteristic peaks in the FT-IR spectra of geopolymer obtained after immersion in chloride and sulfate environments given in Fig.6b and 6c appeared in the same position which is evidence of resistance of geopolymer. These observations prove that the basic structure of a geopolymer is not affected by aggressive environments.

#### *SEM analysis*

SEM micrograph of geopolymer samples has Si to Al ratio of 1.5 before and after immersion in 8 wt.% sodium chloride and sodium sulfate solutions are depicted in Fig. 7. Before immersion, the SEM image given in Fig. 7a is characterized by a smooth and uniform morphology comprising of few clay flakes that are observed to be embedded and bound to the surface. Fig. 7b and 7c demonstrate the effect of chloride and sulfate attack, respectively on morphological features of the geopolymer samples. The sulfate attack was found to be more vigorous than the chloride attack, resulting in greater cracks and voids in the microstructure of the geopolymer. Besides, noticeable surface erosion of geopolymer after exposure to chloride and sulfate can be observed. The differences in the SEM images are highlighted with a red circle.



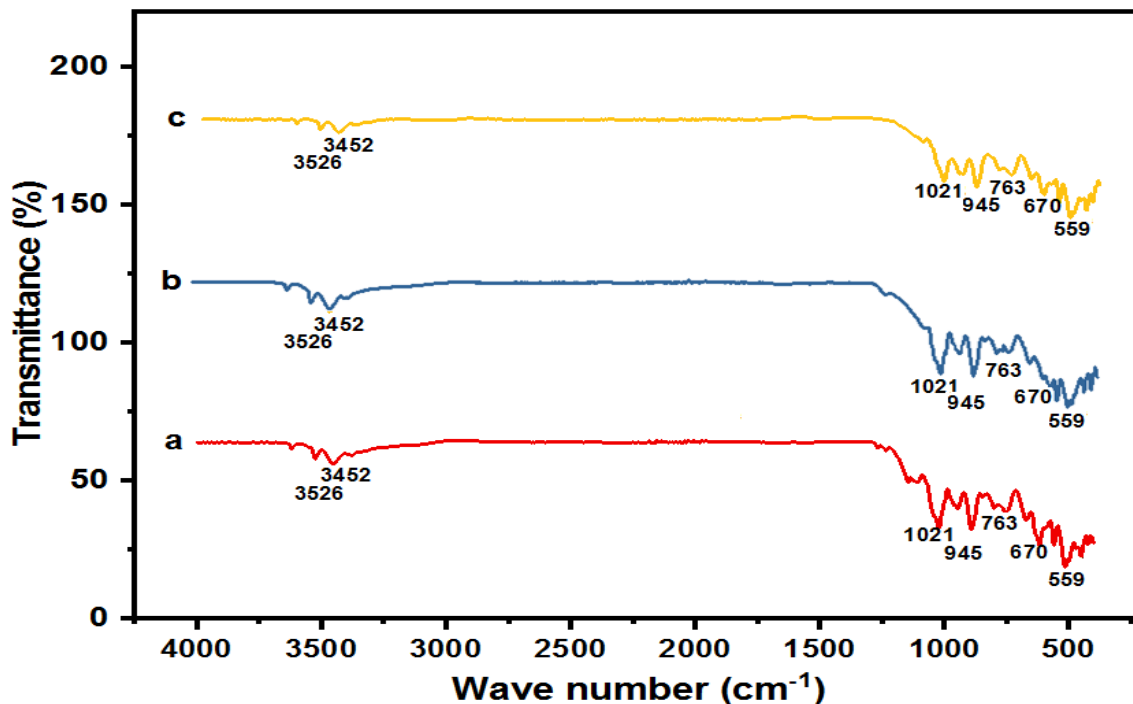


Fig. 6: FT-IR spectra of geopolymer samples: Before immersion (a), after immersion in chloride environment (b) and after immersion in sulfate environment (c).

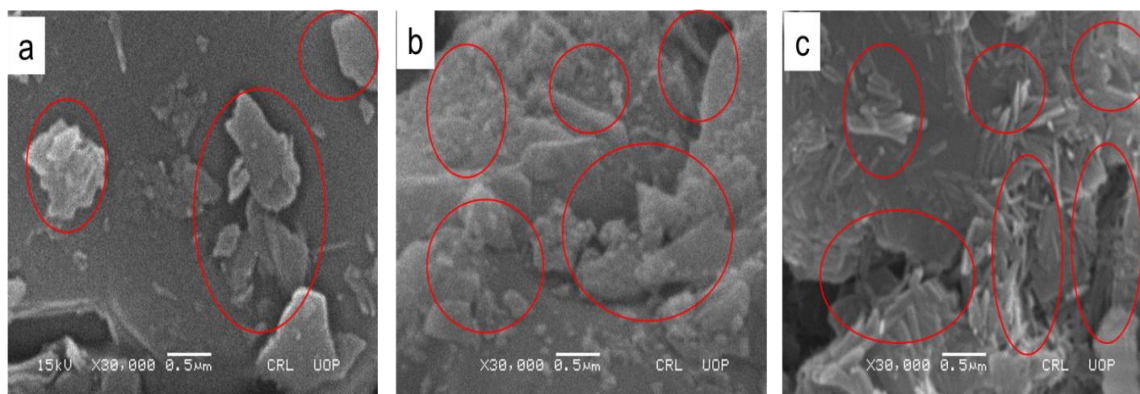


Fig. 7: SEM images of geopolymer samples: Before immersion (a), after immersion in chloride environment (b) and after immersion in sulfate environment (c).

#### XRD analysis

The effect of chloride and sulfate attacks on the basic geopolymer structure was inspected by collecting the X-Ray diffractograms of the geopolymer samples. Fig. 8 shows the diffractograms of specimens before and after immersion in aggressive environments. The XRD pattern provided in Fig. 8a is characterized by zeolite ( $\text{NaAlSi}_2\text{O}_6 \cdot \text{H}_2\text{O}$ ), quartz ( $\text{SiO}_2$ ), hematite ( $\text{Fe}_2\text{O}_3$ ), sodalite ( $\text{Na}_4\text{Al}_3\text{Si}_3\text{O}_{12}\text{Cl}$ ), and almandite ( $\text{Fe}_3\text{Al}_2(\text{SiO}_4)_3$ ) peaks. The existence of

quartz peaks is due to their resistance to dissolve in an alkaline medium and act as fillers [19]. The presence of a hump between  $8$  and  $18^\circ 2\theta$  confirms the amorphous nature of the geopolymer [32]. After the exposure of geopolymer to aggressive environments, no subtle variations can be observed XRD peaks both for crystalline as well as amorphous features of the product. These interpretations proved that the main structure of the geopolymer is not affected by the chloride and sulfate solution even for an exposure period of 35 days.

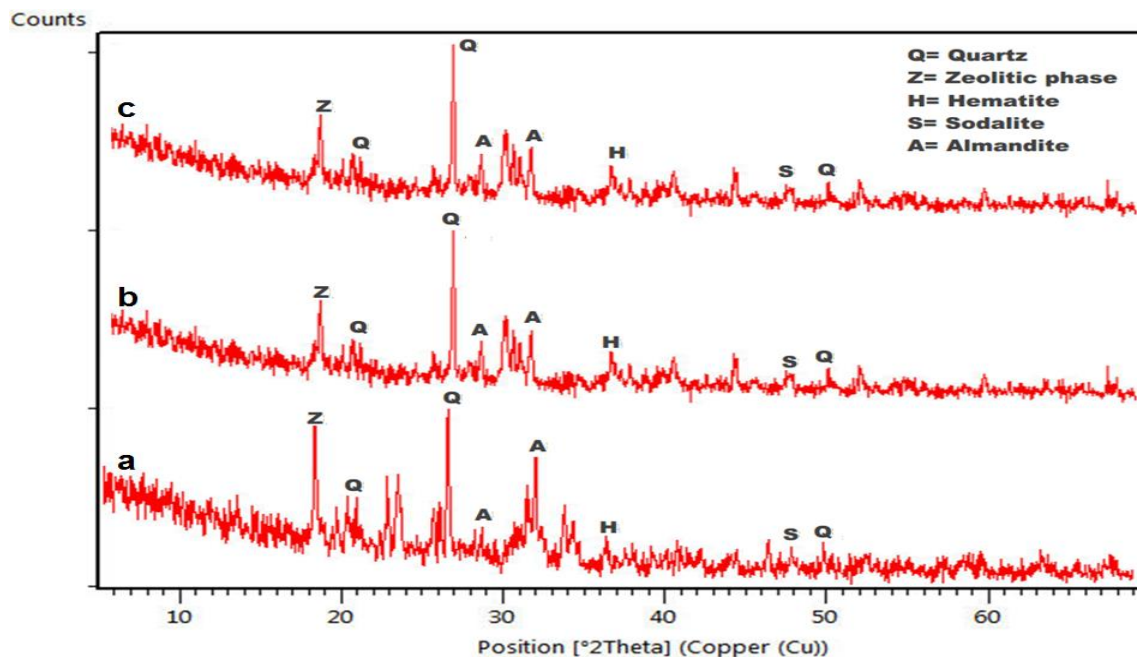


Fig. 8: XRD patterns of geopolymer samples: Before immersion (a), after immersion in chloride environment (b) and after immersion in sulfate environment (c).

### Conclusions

The current study was aimed to report the production of good quality geopolymer from calcined lateritic clay, sodium metasilicate, and aluminum hydroxide and its resistance to the aggressive environment of chloride and sulfate. The following conclusions were drawn from the discussed results:

- FT-IR, XRD, and SEM analyses proved that lateritic clay calcined at 900 °C can be used as a suitable material for geopolymer production.
- The geopolymer sample with a Si to Al ratio of 1.5 shows the highest compressive strength (22.4 MPa) and greater resistance to aggressive environments.
- The resistance offered by the geopolymer sample is found better for sodium chloride than sodium sulfate.
- The effect of chloride and sulfate attack on the main structure of geopolymer having optimum Si to Al ratio found negligible, proved by FT-IR and XRD peaks.

### Acknowledgment

The authors of this research work are thankful to the Centralized Research Laboratory (CRL), University of Peshawar, Department of Chemistry Abdul Wali Khan University Mardan, Department of Chemistry Government Postgraduate College Nowshera, and Department of Chemistry School of Natural Sciences National University of Science and Technology (NUST) Islamabad.

### References

1. N. U. Amin, L. Nawab, and U. Ghani, Synthesis and characterization of chloride resistant cement from industrial waste through geopolymerization, *J. Clean. Prod.*, **156**, 577 (2017).
2. N. B. Singh, M. Kumar, and S. Rai, Geopolymer cement and concrete: Properties, *Mater. Today: Proc.*, (2020).
3. C. Tennakoon, A. Shayan, J. G. Sanjayan, and A. Xu, Chloride ingress and steel corrosion in geopolymer concrete based on long term tests, *Mater. Des.*, **116**, 287 (2017).
4. D. Ren, C. Yan, P. Duan, Z. Zhang, L. Li, and Z. Yan, Durability performances of wollastonite, tremolite and basalt fiber-reinforced metakaolin geopolymer composites under sulfate and chloride attack, *Constr. Build. Mater.*, **134**, 56 (2017).
5. S. Kumar and R. Kumar, Mechanical activation of fly ash: Effect on reaction, structure and properties of resulting geopolymer, *Ceramics International*, **37**, 533 (2011).
6. M. A. M. Ariffin, M. A. R. Bhutta, M. W. Hussin, M. Mohd Tahir, and N. Aziah, Sulfuric acid resistance of blended ash geopolymer concrete, *Constr. Build. Mater.*, **43**, 80 (2013).
7. E. Prud'homme, P. Michaud, E. Joussein, C. Peyratout, A. Smith, and S. Rossignol, In situ inorganic foams prepared from various clays at low temperature, *Appl. Clay Sci.*, **51**, 15 (2011).



8. M. Babae and A. Castel, Chloride-induced corrosion of reinforcement in low-calcium fly ash-based geopolymer concrete, *Cem. Concr. Res.*, **88**, 96 (2016).
9. J. G. D. Nemaleu, R. C. Kaze, S. Tome, T. Alomayri, H. Assaedi, E. Kamseu, U. C. Melo, and V. M. Sglavo, Powdered banana peel in calcined halloysite replacement on the setting times and engineering properties on the geopolymer binders, *Constr. Build. Mater.*, **279**, 122480 (2021).
10. C. R. Kaze, P. Venyite, A. Nana, D. N. Juvenal, H. K. Tchakoute, H. Rahier, E. Kamseu, U. C. Melo, and C. Leonelli, Meta-halloysite to improve compactness in iron-rich laterite-based alkali activated materials, *Mater. Chem. Phys.*, **239**, 122268 (2020).
11. R. Y. Nkwaju, J. N. Y. Djobo, J. N. F. Nouping, P. W. M. Huisken, J. G. N. Deutou, and L. Courard, Iron-rich laterite-bagasse fibers based geopolymer composite: Mechanical, durability and insulating properties, *Appl. Clay Sci.*, **183**, 105333 (2019).
12. J. G. D. Nemaleu, V. Bakaine Djaoyang, A. Bilkissou, C. R. Kaze, R. B. E. Boum, J. N. Y. Djobo, P. Lemougna Ninla, and E. Kamseu, Investigation of Groundnut Shell Powder on Development of Lightweight Metakaolin Based Geopolymer Composite: Mechanical and Microstructural Properties, *Silicon*, (2020).
13. O. F. Nnaemeka and N. B. Singh, Durability properties of geopolymer concrete made from fly ash in presence of Kaolin, *Mater. Today: Proc.*, (2020).
14. A. A. Tigue, R. A. Malenab, J. Dungca, D. Yu, and M. A. Promentilla, Chemical Stability and Leaching Behavior of One-Part Geopolymer from Soil and Coal Fly Ash Mixtures, *Minerals*, **8**, 411 (2018).
15. J. Kwasny, T. A. Aiken, M. N. Soutsos, J. A. McIntosh, and D. J. Cleland, Sulfate and acid resistance of lithomarge-based geopolymer mortars, *Constr. Build. Mater.*, **166**, 537 (2018).
16. G. Lavanya and J. Jegan, Durability Study on High Calcium Fly Ash Based Geopolymer Concrete, *Adv. Mater. Sci. Eng.*, **2015**, 731056 (2015).
17. K. W. Shah and G. F. Huseien, Bond strength performance of ceramic, fly ash and GBFS ternary wastes combined alkali-activated mortars exposed to aggressive environments, *Constr. Build. Mater.*, **251**, 119088 (2020).
18. D. Yan, C. Shikun, J. Jin, Z. Xiuyu, J. Wang, and Q. Zeng, Chemical-physical-mechanical stability of MKG mortars under sulfate attacks, *Adv. Cem. Res.*, **33**, 1 (2020).
19. R. C. Kaze, L. M. Beleuk à Mougam, M. L. Fonkwe Djouka, A. Nana, E. Kamseu, U. F. Chinje Melo, and C. Leonelli, The corrosion of kaolinite by iron minerals and the effects on geopolymerization, *Appl. Clay Sci.*, **138**, 48 (2017).
20. ASTM C311, Standard Test Methods for Sampling and Testing Fly Ash or Natural Pozzolans for Use in Portland-Cement Concrete.
21. C. Nobouassia Bewa, H. K. Tchakouté, D. Fotio, C. H. Rüscher, E. Kamseu, and C. Leonelli, Water resistance and thermal behavior of metakaolin-phosphate-based geopolymer cements, *J. Asian Ceram. Soc.*, **6**, 271 (2018).
22. H. Douiri, S. Louati, S. Baklouti, M. Arous, and Z. Fakhfakh, Structural, thermal and dielectric properties of phosphoric acid-based geopolymers with different amounts of H<sub>3</sub>PO<sub>4</sub>, *Mater. Lett.*, **116**, 9 (2014).
23. N. U. Amin, M. Faisal, K. Muhammad, and S. Gul, Synthesis and characterization of geopolymer from bagasse bottom ash, waste of sugar industries and naturally available china clay, *J. Clean. Prod.*, **129**, 491 (2016).
24. H. Liu, T. Chen, X. Zou, C. Qing, and R. L. Frost, Thermal treatment of natural goethite: Thermal transformation and physical properties, *Thermochim. Acta*, **568**, 115 (2013).
25. A. Hajimohammadi, J. L. Provis, and J. S. J. van Deventer, One-Part Geopolymer Mixes from Geothermal Silica and Sodium Aluminate, *Ind. Eng. Chem. Res.*, **47**, 9396 (2008).
26. Ö. Ahmet and B. K. Mehmet, Evaluation of sulfate and salt resistance of ferrochrome slag and blast furnace slag-based geopolymer concretes, *Struct. Conc: Journal of the fib*, **20**, 1607 (2019).
27. M. Jin, Z. Zheng, Y. Sun, L. Chen, and Z. Jin, Resistance of metakaolin-MSWI fly ash based geopolymer to acid and alkaline environments, *J. Non Cryst. Solids*, **450**, 116 (2016).
28. N. A. Jaya, L. Yun-Ming, H. Cheng-Yong, M. M. A. B. Abdullah, and K. Hussin, Correlation between pore structure, compressive strength and thermal conductivity of porous metakaolin geopolymer, *Constr. Build. Mater.*, **247**, 118641 (2020).
29. S. Alehyen, M. EL Achouri, and M. Taibi, Characterization, microstructure and properties of fly ash-based geopolymer, *J. Mater. Environ. Sci.*, **8**, 1783 (2017).
30. Y.-M. Liew, C.-Y. Heah, A. B. Mohd Mustafa, and H. Kamarudin, Structure and properties of clay-based geopolymer cements: A review, *Prog. Mater. Sci.*, **83**, 595 (2016).
31. F. Ahangaran, A. Hassanzadeh, and S. Nouri, Surface modification of Fe<sub>3</sub>O<sub>4</sub>@SiO<sub>2</sub> microsphere by silane coupling agent, *Int. Nano Lett.*, **3**, 23 (2013).
32. M. Zhang, T. El-Korchi, G. Zhang, J. Liang, and M. Tao, Synthesis factors affecting mechanical properties, microstructure, and chemical composition of red mud-fly ash based geopolymers, *Fuel*, **134**, 315 (2014).